Supporting Information

Patzek et al. 10.1073/pnas.1313380110

SI Text

Here, we describe the role of natural gas in the US economy, describe the details of our data-fitting procedures, provide additional evidence concerning the correspondence of the dimensionless recovery factor (RF) and well production data, provide upper and lower bounds on gas production from wells not yet showing interference, demonstrate why production declines as the square root of time early on and exponentially later, and tabulate the coefficient κ for a variety of reservoir and well flowing pressures to demonstrate how little it varies. In a separate spreadsheet (Dataset S1), we provide tabulations of the dimensionless RF.

Impacts of Natural Gas Production in the United States

As shown in Fig. S1, the United States has managed to maintain gas production at an essentially flat rate for 40 y after a 1974 peak of gas production that closely followed the 1971 peak in oil production. No other country has done the same. Novel technology, most recently the massively hydrofractured horizontal wells in shale plays, has played a crucial role in maintaining US gas production at or slightly above its 1974 level. As a result of plentiful gas production, US gas prices have recently been a fraction of the typical world gas prices, injecting over half a trillion current dollars into the US economy (Fig. S2). This "second stimulus package" in the United States has been almost invisible to the public.

Data Analysis and Fitting Procedure

We analyzed the 16,533 wells in our dataset for the Barnett Shale through the following steps:

i) We eliminate all wells that have been recompleted, all vertical wells, and all months from each well's time history with production of zero. At this point, 11,566 wells remain.

ii) We eliminate all wells with less than 18 mo of total production. Now, 8,807 wells remain.

iii) For each well, we have a measurement of production per day for a sample of days each month. We convert to production per month by multiplying by 30.4.

iv) The first 3 to 4 mo of production are typically noisy and sporadic, particularly because hydrofracturing water is still being back-produced. Therefore, from the time series for each well, we construct a slightly modified one. We label the starting time of this new series 2.5 (mo), and we assign to it the cumulative production of the first 4 mo. There is no further processing: For each new nonzero gas volume produced in a given month, time increases by 1 mo and cumulative production increases by the production of that month until the data end.

v) We use the Levenberg–Marquardt least-squares minimization (lmfit) Python package to find the values of the interference time τ and gas in place $\mathcal{M}$ that best fit our scaling curve to the measured cumulative production. In particular, we minimize the objective function $\mathbf{m}(t) - \mathcal{M}\mathrm{RF}(t/\tau)$, where $\mathbf{m}(t)$ is the measured cumulative production data. Although the reservoir pressure p_i is not the same for all wells in the Barnett Shale, we make use only of the curve corresponding to $p_i = 3{,}500$ psi, $p_f = 500$ psi in this paper. We also conducted the analysis allowing p_i to vary according to measured pressure variations, but the difference was negligible.

vi) We had to guard against a number of artifacts that could produce spurious agreement between well histories and the scaling function. For wells with very short histories, fluctuations in production could produce shapes that mimicked large segments or small portions of the scaling curve. We eliminated these matches by requiring at least 18 mo of production and requiring well histories to traverse a considerable portion of the scaling function rather than running tangent to it over a brief interval. In total, 513 wells were eliminated in this way, leaving 8,294 wells. In no case did we eliminate any well history because its fit to the scaling function was poor. Our plots include all wells except for those whose history was too short to include for the reasons we describe.

vii) An advantage of the lmfit package is that it includes careful estimates of the uncertainty of parameters. We used the routine conf_interval to improve the estimates. Our scaling curve $\mathrm{RF}(\tilde{t})$ is practically indistinguishable from a square root until the argument $\tilde{t}$ approaches 1. Thus, it is impossible to obtain a useful estimate of the interference time and gas in place unless interference has become visible. To select a quantitative criterion, we found that the average uncertainty of the parameters τ and $\mathcal{M}$ was more than 20% unless the scaled age of the well, $t_{\max}/\tau$, was greater than around 0.64. Accordingly, we used the condition $\tilde{t}_{\max} > 0.64$ to divide wells into two groups. Careful analysis of the magnitude of the objective function as a function of the fitting parameters $\mathcal{M}$ and τ indicates that these uncertainty estimates are somewhat too tight. There is a narrow valley in τ-$\mathcal{M}$ space, where the function varies very slowly on large scales but has relatively rapidly varying local minima on shorter scales. The uncertainty estimates could probably be improved and would become somewhat larger by taking into account these adjacent local minima, but we have not yet done this.
We found a small number of wells with interference times less than 1 y, probably because of the high-permeability channels leading to interactions of hydrofractures or hydrofracture branches that are very close to each other.

viii) For wells with $\tilde{t}_{\max} > 0.64$ and $\tilde{t}_{\min} < 0.25$, we estimate τ and $\mathcal{M}$. The result appears in Fig. 4. The interference times are short as they must be; because such horizontal wells are, at most, 14 y old and most are younger, it is impossible to detect interference times of much more than 10 y, and the typical measured interference time is only 5 y.

ix) For wells with $\tilde{t}_{\max} < 0.64$, the estimates of τ and $\mathcal{M}$ are too uncertain to be useful, but we can provide bounds. The lower bound on τ is obtained from the observation that interference would be visible if $\tilde{t}_{\max}$ were greater than 0.64. Because it is not visible, one must have $\tilde{t}_{\max} = t_{\max}/\tau < 0.64 \Rightarrow \tau > t_{\max}/0.64$.

x) For wells that do not show interference, the constant $\mathcal{K}$ from Eq. **6** can be determined from the data and the lower bound on τ can be converted into a lower bound on $\mathcal{M}$.

xi) A reasonable upper bound on $\mathcal{M}$ can be obtained from data on the size of each well and the thickness of the mudrock layer (1). The upper bound on $\mathcal{M}$ can be converted into an upper bound on τ using Eq. **6.**

Additional Checks on RF

We provide two additional checks on the scaling function formalism. First, we check whether production rates for wells showing evidence of interference do indeed decline exponentially. Evidence is provided in Fig. S3. Although rates are very noisy, with many months where production drops by a large factor and recovers, as well as occasional excursions above the predicted curve, overall rates decline in accord with the predicted exponential.

Second, we check in Fig. S4 whether the measurement of the original gas in place $\mathcal{M}$ obtained from the scaling formalism is bounded above by estimates obtained from data on the extent of the well. The two measurements are coming from separate data sources, so the comparison is a strong test of both data integrity and the sense of our formalism. The estimated gas in place of virtually every well lies below the upper bound. In addition, the information coming from the scaling formalism is not redundant because the measurement of $\mathcal{M}$ obtained in this way is usually considerably less than the upper bound.

Upper and Lower Bounds on Gas Production from Wells in Square Root Phase

Fig. S5 provides four additional pieces of information for the wells that show no evidence of interference. In the Fig. S5 (*Upper Left),* we provide a lower bound on the interference time τ. This lower bound is obtained by noting that interference becomes evident when $\tilde{t}$ reaches 0.64, so if interference is not evident, the interference time τ must be at least 1.6 times larger than the current life of the well. From this estimate one obtains a lower bound on the gas in place for each well, since Eq. **6** and the known value of $\mathcal{K}$ for each well turns a lower bound on τ into a lower bound on $\mathcal{M}$ (Fig. S5, *Upper Right*). Fig. S5 (*Lower Right*) displays an upper bound on the original gas in place $\mathcal{M}$ obtained by using the measured thickness of the mudstone source rock of each well, and the length of the well. From the upper bound on $\mathcal{M}$ one obtains through Eq. **6** an upper bound on τ, shown in the lower left. This bound on τ is not very tight. There is a peak at around 30 y, but a long tail stretching into the hundreds of years. We think it is impossible that wells will last this long before beginning to interfere, but they are simply too young to provide evidence that interference will occur any sooner.

Asymptotic Analysis of Gas Production at Early Times

For a domain bounded on two sides, as in Fig. 1, the diffusion equation (Eq. **21**) must be solved numerically. However, if the boundary conditions are changed so that $\tilde{m}$ vanishes at $x=0$ and $\tilde{m}\to\tilde{m}_i$ as $x\to\infty$, then as pointed out by Crank and Henry (2), this equation possesses an exact similarity solution.

To find this solution, let

$$\eta \equiv \frac{x}{\sqrt{t}}. \qquad \textbf{[S1]}$$

Then Eq. **21** becomes

$$-\frac{1}{2}\frac{\partial\tilde{m}}{\partial\eta}\eta = \frac{\alpha}{\alpha_i}\frac{\partial^2\tilde{m}}{\partial\eta^2}. \qquad \textbf{[S2]}$$

This equation is of the first order in $\partial\tilde{m}/\partial\eta$, and the solution is obtained in a straightforward manner. Define $\mathcal{F}$ by

$$\mathcal{F}(\eta) = \int_0^\eta d\eta' \exp\left(-\frac{\alpha_i}{2}\int_0^{\eta'} d\eta'' \frac{\eta''}{\alpha(\eta'')}\right). \qquad \textbf{[S3]}$$

Then

$$\tilde{m}(\eta) = m_i \frac{\mathcal{F}(\eta)}{\mathcal{F}(\infty)}. \qquad \textbf{[S4]}$$

This equation appears at first to be an explicit expression in closed form, but because $\alpha(\eta)$ is, in fact, $\alpha[m(\eta)]$, it is actually an integral equation whose solution must be determined self-consistently. An important result that can nevertheless be obtained from it is that

$$\left.\frac{\partial\tilde{m}}{\partial\tilde{x}}\right|_0 = \frac{1}{\sqrt{\tilde{t}}}\frac{m_i}{\mathcal{F}(\infty)}. \qquad \textbf{[S5]}$$

Thus, mass transport due to this similarity solution has the exact property of decaying in time as $1/\sqrt{t}$. The coefficient of the decay can only be determined through integrals over the complete spatial solution. Cumulative production is given by the time integral, and goes as $\sqrt{t}$.

For any given initial condition, solutions of the diffusion equation (Eq. **21**) in a semiinfinite space tend toward the solution given in Eq. **S4**. This is why, after an early transient period, decline of production as $1/\sqrt{t}$ and growth of cumulative production as $\sqrt{t}$ are universal for a time. This solution persists until the onset of interference between consecutive hydrofractures.

Asymptotic Analysis of Gas Production at Late Times

When one waits sufficiently long, pressure drops everywhere in the reservoir until it hovers just above the well flowing pressure. In this late-time regime, the hydraulic diffusivity $\alpha(p)$ can be replaced by the constant $\alpha\equiv\alpha(p_f)$. With the simplification that the hydraulic diffusivity α is constant and the interference time τ and scaled time $\tilde{t}$ are defined in terms of α, Eq. **21** can be solved exactly with the same boundary conditions as before, and the result is

$$\left.\frac{\partial\tilde{m}}{\partial\tilde{x}}\right|_0 = 2\sum_{n=0}^{\infty} \mathrm{e}^{\left(-(2n+1)^2\pi^2\tilde{t}/4\right)} \approx \underbrace{\frac{\sqrt{\pi}\,\mathrm{erfc}\left(3\sqrt{\pi^2\tilde{t}/4}\right)}{4\sqrt{\pi^2\tilde{t}/4}}}_{\text{“Hyperbolic” or square root of time decline}} + \underbrace{e^{-\pi^2\tilde{t}/4} + \frac{1}{2}e^{-9\pi^2\tilde{t}/4}}_{\text{Exponential decline}}. \qquad \textbf{[S6]}$$

The relative importance of the three terms in Eq. **S6** is plotted in Fig. S5. We make two points about the result.

i) If the only goal is to provide an accurate account of the long-time behavior, this computation shows self-consistently that the decline rate is exponential just so long as the limit of α as $p\to p_f$ is well defined.

ii) One can instead use the computation as an approximate analytical description of the entire decline process. In this case, instead of using $\alpha=\alpha(p_f)$, one should use $\alpha=\alpha(\overline{p})$; that is, one should use a hydraulic diffusivity characteristic of the average pressure in the reservoir. The resulting approximation has the property of leading to a decline curve that goes as $1/\sqrt{t}$ at early times, and declining exponentially at late times just like the exact solution (Fig. S6). However, this approximation leads to errors on the order of 50%. No matter how one tunes a constant α, one cannot get both the coefficient of the original $1/\sqrt{t}$ decline and the total gas recovered right.

Tabulation of κ

Table S1 extracts the coefficient κ, describing the initial rise in cumulative production as $\kappa\sqrt{\tilde{t}}$ from the dimensionless RF for a variety of reservoir and well flowing pressures. The main lesson is that it varies rather little and can safely be taken to assume a nominal value of 0.645 across the Barnett Shale.

1. Fu Q, et al. (2013) Log-based thickness and porosity mapping of the Barnett Shale play, Fort Worth Basin, Texas: A proxy for reservoir quality assessment. *AAPG Bull*, in press.

2. Crank J, Henry ME (1949) Diffusion in media with variable properties. *Transactions of the Faraday Society* 45:636–650.

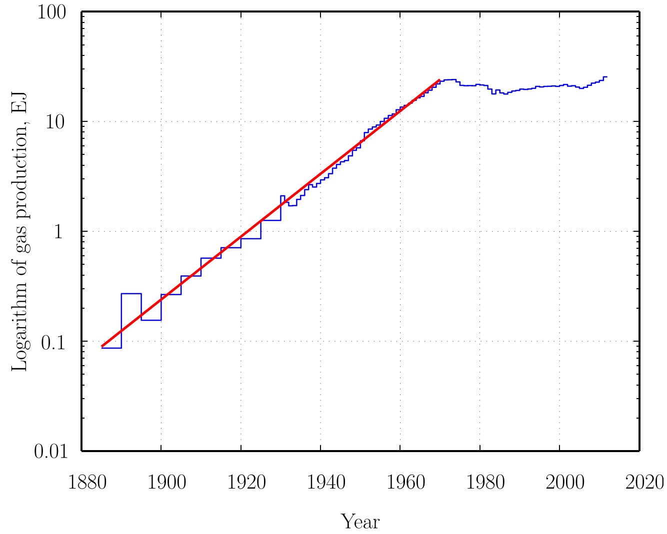

Fig. S1. In the United States, gas production doubled about 10-fold, growing by a factor of ∼1,000. Natural gas production, associated with the fundamental Hubbert oil peak in the United States, peaked in 1974. However, a second "fundamental" gas cycle has been created by producing new gas (increasingly deep offshore, from Alaska, tight gas sands, coal-bed methane, and now shales) resources in the United States. As a result, after growing at 7% per year until 1974 (red line), gas production has remained flat over the past 40 y (blue line). Recently, gas production in the United States has actually been increasing, mostly due to shale gas production. Note that 1 exaJoule (EJ) ≈ 1 trillion standard cubic feet (Tscf) of gas. Data source: US Department of Energy, Energy Information Administration.

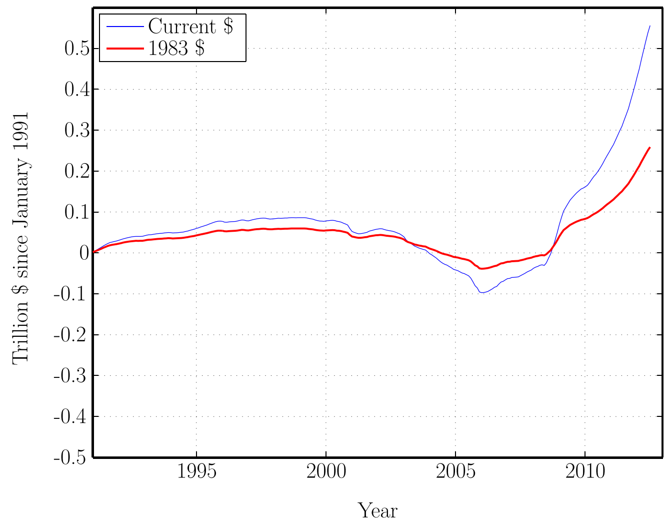

Fig. S2. Because of shale gas production, natural gas prices in the United States have plummeted to one-fourth of the Russian gas price. This plot subtracts the cumulative amount the United States has actually spent on natural gas from the amount it would have spent at world (Russian) prices. Since 1991, domestic gas production in the United States has delivered $560 billion US dollars (blue line) ($250 billion in constant 1983 US dollars, red line) to the US economy. Cheap natural gas has led to a decrease of US CO_2 emissions, increased employment, and a renaissance of steel production and manufacturing. Cheap reliable energy is fundamental to a healthy economy, but very few people recognize this truism. Natural gas prices are from the Index Mundi (www.indexmundi.com/commodities/). The consumer price index is from the US Census Bureau.

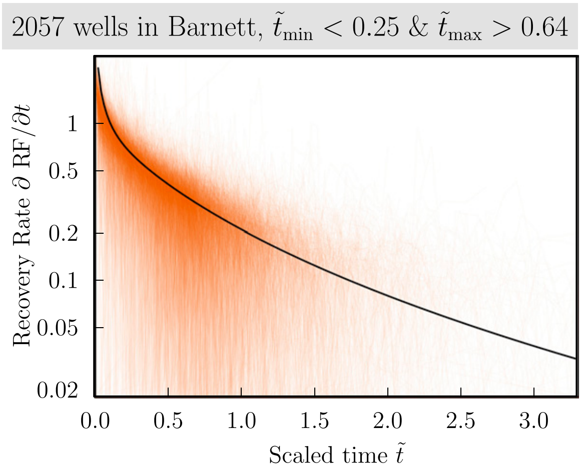

Fig. S3. Production rate for all qualifying horizontal wells in the Barnett Shale shows evidence of interference.

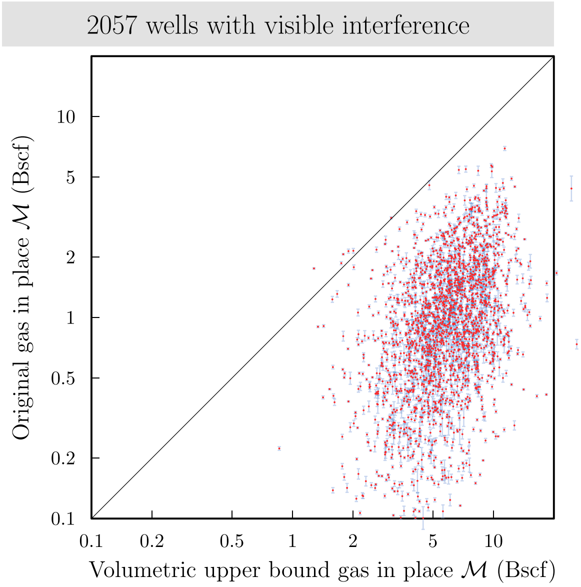

Fig. S4. Original gas in place is computed by fitting $\mathcal{M}$ to well production data compared for each well, with an upper bound obtained from data on the dimensions of the well.

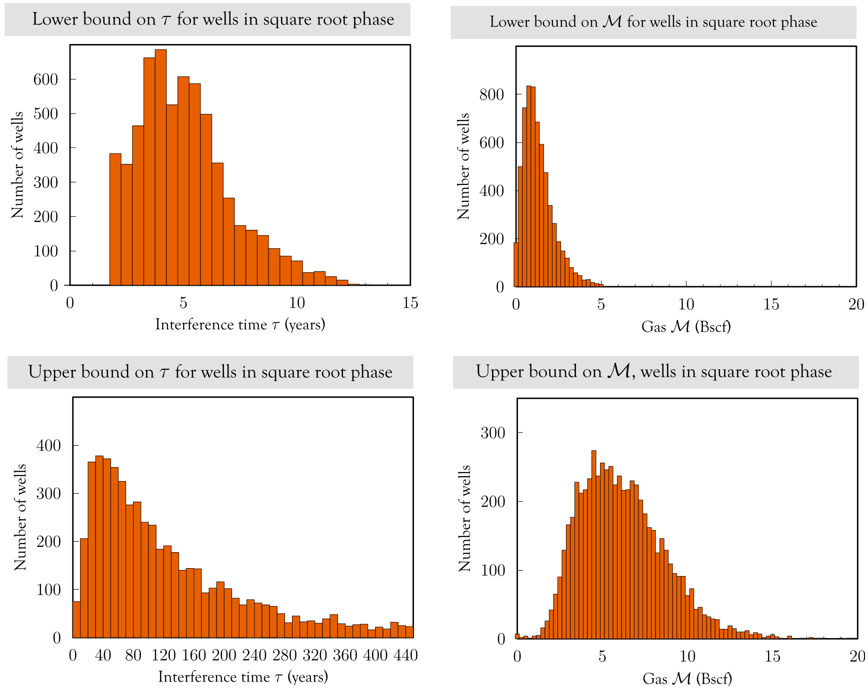

Fig. S5. Bounds on the interference time τ and the original mass of gas in place $\mathcal{M}$ for the wells from Fig. 3*B* in the square root phase.

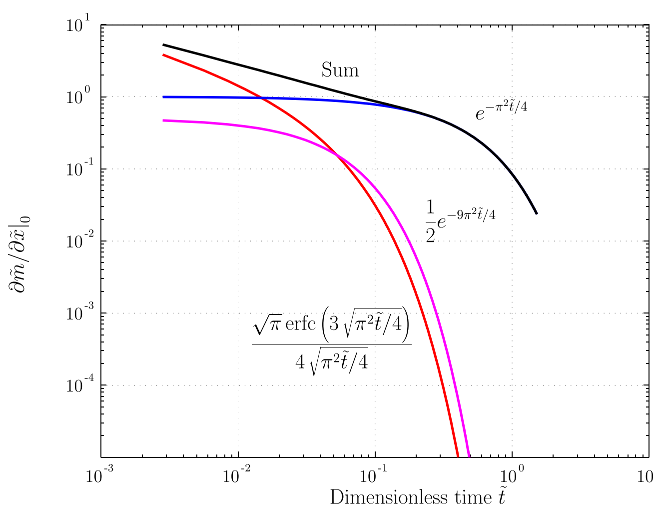

Fig. S6. Relative importance of the three-term rate approximation in Eq. **S6**, summed to form the black curve. Note that for $\tilde{t} \le 0.2$, production declines as the square root of time (red curve). For $\tilde{t} \ge 1$, the production rate decline is exponential (pink and blue curves). For $0.2 \le \tilde{t} < 1$, there is a transition from the square root of time decline to the exponential decline. This plot was obtained from linear analysis. For nonlinear cases, it turns out that when the time to interference, τ, is referenced to the initial reservoir conditions, similar values of $\tilde{t}$ govern transitions between production decline regimes.

Table S1. Scaling factor κ

	$p_f = 500$	$p_f = 400$
p_i	κ	κ
2,000	0.650	0.671
2,500	0.663	0.672
3,000	0.661	0.671
3,500	0.645	0.653
4,000	0.634	0.642
4,500	0.633	0.641

For scaled times $\tilde{t} < 0.2$, cumulative production increases as $\sqrt{\tilde{t}}$. The dimensionless RF $\approx \kappa\sqrt{\tilde{t}}$ and this table display values of κ for various initial and well flowing pressures for a reservoir temperature of 190 °F. There is no simple expression for κ, but it does not vary much.

Other Supporting Information Files

Dataset S1 (XLS)